Design of quarter-wavelength resonator filters with coupling controllable paths

Meng, Fanyi; Ma, Kaixue; Xu, Shanshan; Yeo, Kiat Seng; Boon, Chirn Chye; Lim, Wei Meng; Do, Manh Anh

2012

Meng, F., Ma, K., Xu, S., Yeo, K. S., Boon, C. C., Lim, W. M., & Do, M. A. (2012). Design of quarter-wavelength resonator filters with coupling controllable paths. 2012 IEEE Asia Pacific Conference on Circuits and Systems (APCCAS), pp.248-251.

https://hdl.handle.net/10356/101958

https://doi.org/10.1109/APCCAS.2012.6419018

Design of Quarter-Wavelength Resonator Filters with Coupling Controllable Paths

Fanyi Meng, Kaixue Ma, Shanshan Xu, Kiat Seng Yeo, Chirn Chye Boon, Wei Meng Lim, and Manh Anh Do
School of Electrical and Electronic Engineering
Nanyang Technological University
Singapore 639798
Email: {meng0031, kxma}@ntu.edu.sg

***Abstract*—This paper presents compact quarter-wavelength resonator filters to have multiple transmission zeros points (ZPs) with controllable electric and magnetic coupling paths. For two coupled resonators, the relative strength of electric and magnetic coupling paths determines the transmission ZPs positions that can be at either lower or upper stopband. Besides, the location of transmission ZPs can be precisely controlled by tuning the dimension parameters. Based on the proposed topology and configuration, the second-order and fourth-order bandpass filters operating at 5.1 GHz have been designed using multi-layer LTCC technology.**

I. INTRODUCTION

Filters with compact size, good selectivity, and low cost are one of the key components in RF front-ends. As its advantages in smaller size and lower cost, miniaturized filters have spurred a hot research interest over the past decades. Among various compact filter designs, the use of slow-wave effect [1], dual-mode resonators [2], and multilayer structures [3] are popular. For instance, microstrip slow-wave open-loop resonator filters by using capacitive loaded transmission line was described in [1]. However, this approach is not very practical for large fractional bandwidth filter realization. In [2], a dual-mode microstrip ring resonator filter with two transmission poles and two transmission ZPs was realized in one ring resonator only. But the dual-mode design is more complex in design procedures compared to conventional structure. With the advancement in low temperature co-fired ceramic (LTCC) technology, the multi-layer process can be utilized to reduce the size of planar filters tremendously. For example, a very compact and low-profile LTCC filter with hybrid resonators was demonstrated in [3].

The parallel-coupled half-wavelength resonator filter configuration [4] is commonly used. However, this type of filters occupies large area and suffers spurious from twice the center frequency. In contrast, the quarter-wavelength designs reduce the size with spurious from three times the center frequency.

In order to meet more rigorous specifications from communication technology advancement, the elliptic filters which provide finite transmission ZPs at the real axis can reduce the number of resonators and this in turn, reduces the filter size and manufacturing costs. For planar filter application, a modified short-circuited quarter-wavelength filter with separate electric and magnetic coupling paths has been discussed in [5]. A filter operating at 60 GHz with modified hairpin resonators to realize separate electric and

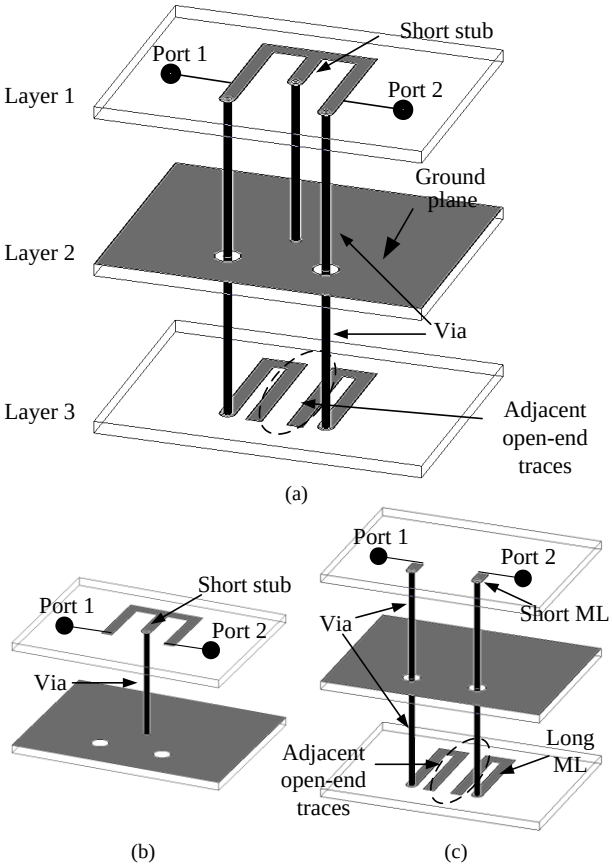

Figure 1. Proposed second-order filter configuration and equivalent circuits: (a) proposed filter, (b) M-path, and (c) E-path.

magnetic coupling paths was also reported in [6]. However, these designs are still large for modern communication system requirements.

In this paper, a quarter-wavelength resonator filter with separate controllable electric and magnetic coupling paths in multi-layer structure is proposed. The configurations of proposed microstrip filters corresponding to electric or magnetic dominant conditions are presented and analyzed. Besides the additional ZPs generation and frequency control of ZPs, the size reduction is more than 50% comparing to same order SEMCP filters in planar realization [5]. The filters with ZPs in lower, upper or both stopband have been designed and discussed.

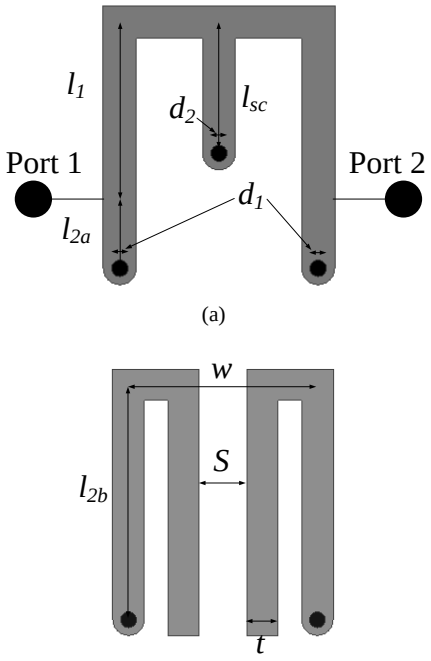

Figure 2. Proposed second-order filter configurations: (a) Layer 1 and (b) Layer 3.

II. Second-Order Filter Realization

The proposed resonator is shown in Fig. 1(a), consisting of two separated parallel coupling paths, i.e. the magnetic coupling path (M-path) in Fig. 1(b) and the electric coupling path (E-path) in Fig. 1(c) formed on three metal layers. Layer 2 acts as the common ground plane. M-path is formed on layer 1 using MLs, short stub, and via hole. E-path comprises of short microstrip lines (MLs) in layer 1, via from layer 1 to layer 3, and long MLs with adjacent open-end traces in layer 3. Since the common ground layer physically separates M- and E-paths and negligible coupling exists in between, the two paths can be controlled separately. Thus, second-order filter with two controllable and separated coupling paths between resonators is realized.

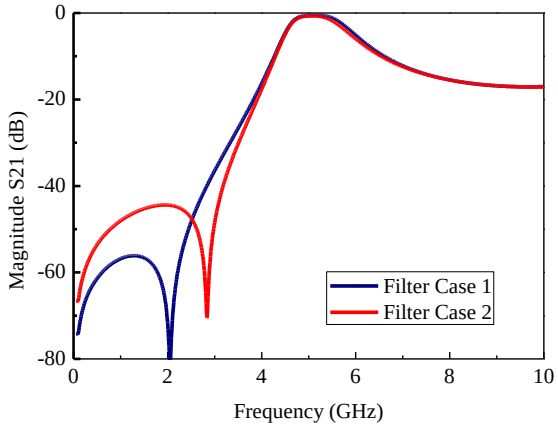

(a)

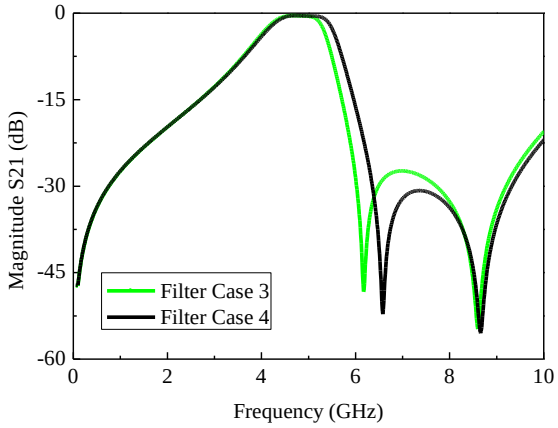

(b)

Figure 3. Transmission characteristics of the filter in Fig. 1: (a) Case 1 and 2; (b) Case 3 and 4.

In Fig. 2, the multi-layer structure in Fig. 1 is detached and shown in planar layers, i.e. layer 1 in Fig. 2(a) and layer 3 in Fig. 2(b) for illustration purposes. Layer 2 is common ground plane with holes for via to go through and is omitted here. From earlier discussion, it is easy to observe that the length of short stub l_{sc} in layer 1 forms inductive (magnetic) coupling and determines the coupling strength in M-path as longer l_{sc} results in stronger magnetic coupling effect. At the same time, the spacing between two adjacent traces S in layer 3 determines the capacitive (electric) coupling strength in E-path as larger S results in weaker electric coupling effect.

The LTCC substrate with relative permittivity of 7.1, loss tangent of 0.005, and dielectric layer thickness of 85 μm is used in analysis and design. The Ansoft HFSS 13.0 is used for full-wave simulation. Four cases in different dimensions are simulated and shown in Fig. 3. The physical parameters of four cases are:

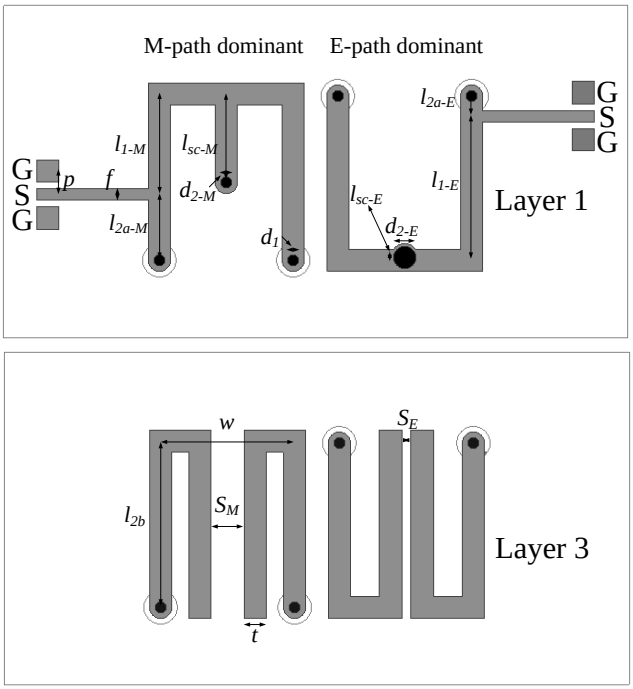

(a)

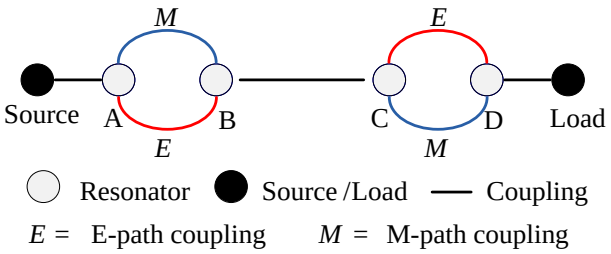

(b)

Figure 4. Proposed fourth-order filter configuration and topology: (a) filter configuration and (b) filter topology.

- Case 1: l_1 = 0.9mm, l_{2a} = 0.6mm, l_{sc} = 0.025mm, S = 0.04mm, l_{2b} = 1.5mm, w = 1.2mm, t = 0.2mm, and via diameters d_1 = 0.1mm, d_2 = 0.2mm.
- Case 2: l_1 = 0.9mm, l_{2a} = 0.6mm, l_{sc} = 0.2mm, S = 0.04mm, l_{2b} = 1.5mm, w = 1.2mm, t = 0.2mm, and via diameters d_1 = 0.1mm, d_2 = 0.2mm.
- Case 3: l_1 = 1.3mm, l_{2a} = 0.2mm, l_{sc} = 0.8mm, S = 0.3mm, l_{2b} = 1.5mm, w = 1.2mm, t = 0.2mm, and via diameters d_1 = 0.1mm, d_2 = 0.2mm.
- Case 4: l_1 = 1.3mm, l_{2a} = 0.2mm, l_{sc} = 0.8mm, S = 0.4mm, l_{2b} = 1.5mm, w = 1.2mm, t = 0.2mm, and via diameters d_1 = 0.1mm, d_2 = 0.2mm.

In Case 1 and 2, the length of short stub l_{sc} and spacing between two adjacent traces S are relatively small that results in weaker coupling in M-path and stronger coupling in E-path.

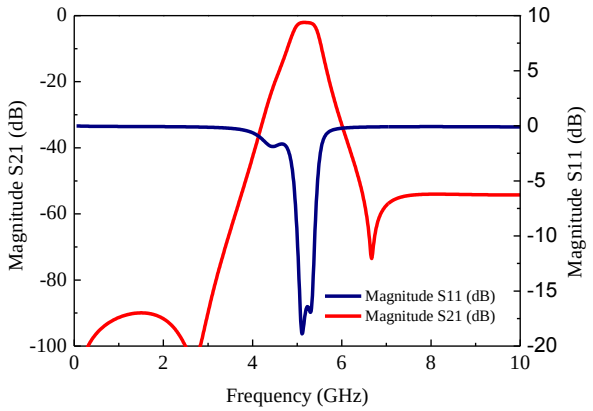

Figure 5. Simulation results of proposed fourth-order filter.

Therefore, the E-path dominates in total coupling effect and a ZP is generated at lower stopband as in Fig. 3(a). Without affecting the passband performance, the transmission ZP is shifted from 2.05 GHz in Case 1 to 2.85 GHz in Case 2 by varying the M-path coupling strength as in Fig. 3(a). Thus, the location of ZP is controllable by tuning the dimension parameter l_{sc}.

In Case 3 and 4, the length of short stub l_{sc} and spacing between two adjacent traces S are relatively large that results in stronger coupling in M-path and weaker coupling in E-path. Therefore, the M-path dominates in total coupling effect and two ZPs are generated at upper stopband as in Fig. 3(b). Comparing Case 3 and Case 4, the first transmission ZP is moved from 6.58 GHz in Case 4 to 6.17 GHz in Case 3 as in Fig. 3(b). It is shown that the location of zero points is also controllable by changing the physical dimension S.

In all the four cases, the full-wave simulated results shows that the operating frequency is 5.1 GHz, insertion loss is better than 0.5 dB, and occupied area is only 1.7 mm × 1.4 mm. The locations of transmission ZPs are controllable to be in either lower or upper stopband. Moreover, the transmission ZPs are capable to be shifted closer to passband so that the filter achieves better roll-off performance. However, it is noted that the filter rejection is poorer as tradeoff in filter designs with ZPs closer to passband.

III. FOURTH-ORDER FILTER REALIZATION

Fig. 4(b) demonstrates the fourth-order filter topology by using separate coupling paths between adjacent resonators. From discussion in Section II, the locations of transmission ZPs are determined by the relative strength in coupling paths. Thus, the dominant E-path coupling can be set in order to generate ZPs in the low stopband, while the dominant M-path coupling can be used to generate ZPs in the upper stopband. If the filter has both dominant E-path and M-path pairs simultaneously, it is believed that the ZPs can be generated in both the lower and upper stopband.

To demonstrate the control of ZPs both in the lower and upper stopband, the configuration of fourth-order filter with

one M-path dominant pair and one E dominant pair in Fig. 4(a) is simulated and studied. Two separate coupling paths with dominant M-path coupling are introduced between resonators A and B and dominant E-path coupling between resonators C and D. The external quality factor and the inter-stage coupling coefficients can be calculated as in [7]. The dimensions are set to be*:* $l_{1\text{-}M}$ = 0.9mm, $l_{1\text{-}E}$ = 1.3mm, $l_{2a\text{-}M}$ = 0.6mm, $l_{2a\text{-}E}$ = 0.2mm, d_1 = 0.1mm, $d_{2\text{-}M}$ = 0.1mm, $d_{2\text{-}E}$ = 0.2mm, $l_{sc\text{-}M}$ = 0.8mm, $l_{sc\text{-}E}$ = 0.025mm, f = 0.1mm, p = 0.15mm, S_M = 0.3mm, S_E = 0.08mm, l_{2b} = 1.5mm, w = 1.2mm and t = 0.2mm. The ground-signal-ground (GSG) pads with 150 μm pitches are co-designed for on-chip measurement, which are connected to vector network analyzer for obtaining scattering parameters.

The simulation results are shown in Fig. 5. The filter is operating at 5.1 GHz, with a 3-dB fractional bandwidth of 12% and insertion loss of 2.1 dB. The ZPs are located at 2.7 and 6.7 GHz. The filter occupies only 1.7 mm × 3 mm ($0.0785\lambda_g \times 0.1385\lambda_g$), achieving size reduction of 67% in terms of λ_g^2 comparing to fourth-order SEMCP filter ($0.192\lambda_g \times 0.174\lambda_g$) in [5] ($\lambda_g$ is the guided wavelength at operating frequency).

IV. Conclusion

In this paper, a multi-layer bandpass filter with separated coupling paths is proposed and implemented based on LTCC technology. Two kinds of second-order filters with transmission ZPs on lower or upper stopband and a fourth-order filter with controllable transmission ZPs in both lower and upper stopband are designed. The filters achieve good selectivity, sharp roll-off and compact size. The transmission ZPs generation and the coupling characteristics are also studied.

References

[1] J. S. Hong and M. J. Lancaster, "Theory and experiment of novel microstrip slow-wave open-loop resonator filters," *IEEE Trans. Microw. Theory Tech.*, vol. 45, no. 12, pp. 2358-2365, Dec. 1997.

[2] U. Karacaoglu, I. D. Robertson, and M. Guglielmi, "An improved dual-mode microstrip ring resonator filter with simple geometry," in *Proc. Eur. Microw. Conf.*, pp. 472-477, 1994.

[3] M. Tamura, T. Yang, and T. Itoh, "Very compact and low-profile LTCC unbalanced-to-balanced filters with hybrid resonators," *IEEE Trans. Microw. Theory Tech.*, vol.59, no.8, pp.1925-1936, Aug. 2011.

[4] S. B. Cohn, "Parallel-coupled transmission-line-resonator filters," *IRE Trans. Microw. Theory Tech*., vol. 6, no. 4, pp. 223–231, Apr. 1958.

[5] K. Ma, J.-G. Ma, K. S. Yeo, and M. A. Do, "A compact size coupling controllable filter with separated electric and magnetic coupling paths," *IEEE Trans. Microw. Theory Tech*., vol. 54, no. 3, pp. 1113-1119, Mar. 2006.

[6] F. Meng, K. Ma, K. S. Yeo, S. Xu, and M. Nagarajan, "A compact 60 GHz LTCC microstrip bandpass filter with controllable transmission zeros," *International Conf. of Electron Devices and Solid-State Circuits (EDSSC)*, pp.1-2, 17-18 Nov. 2011.

[7] J. S. Hong and M. J. Lancaster, *Microstrip Filters for RF/Microwave Applications*. New York: Wiley, 2001, ch. 10, pp. 315-377.